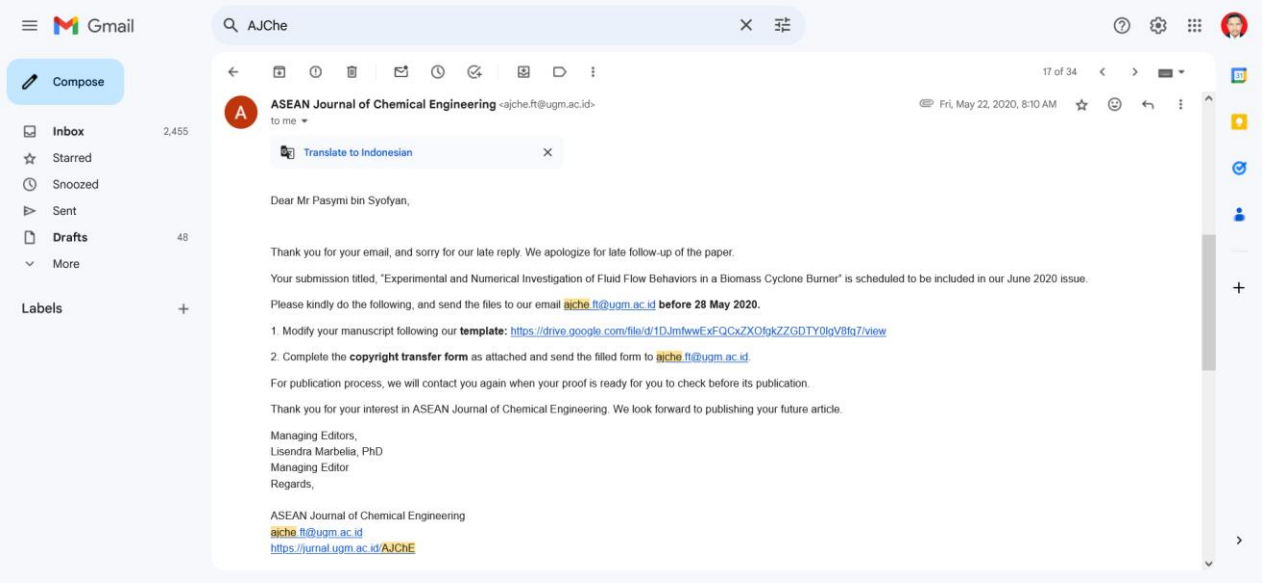
Gmail
AJChe
Compose
Inbox 2,455
Starred
Snoozed
Sent
Drafts 48
More
Labels
17 of 34
ASEAN Journal of Chemical Engineering <ajche.ft@ugm.ac.id>
to me
Fri, May 22, 2020, 8:10 AM
Translate to Indonesian
Dear Mr Pasymi bin Syofyan,
Thank you for your email, and sorry for our late reply. We apologize for late follow-up of the paper.
Your submission titled, "Experimental and Numerical Investigation of Fluid Flow Behaviors in a Biomass Cyclone Burner" is scheduled to be included in our June 2020 issue.
Please kindly do the following, and send the files to our email ajche.ft@ugm.ac.id before 28 May 2020.
1. Modify your manuscript following our template: https://drive.google.com/file/d/1DJmfwwExFQCxZXOfgkZZGDTY0lgV8fq7/view
2. Complete the copyright transfer form as attached and send the filled form to ajche.ft@ugm.ac.id.
For publication process, we will contact you again when your proof is ready for you to check before its publication.
Thank you for your interest in ASEAN Journal of Chemical Engineering. We look forward to publishing your future article.
Managing Editors,
Lisendra Marbelia, PhD
Managing Editor
Regards,
ASEAN Journal of Chemical Engineering
ajche.ft@ugm.ac.id
https://jurnal.ugm.ac.id/AJChE

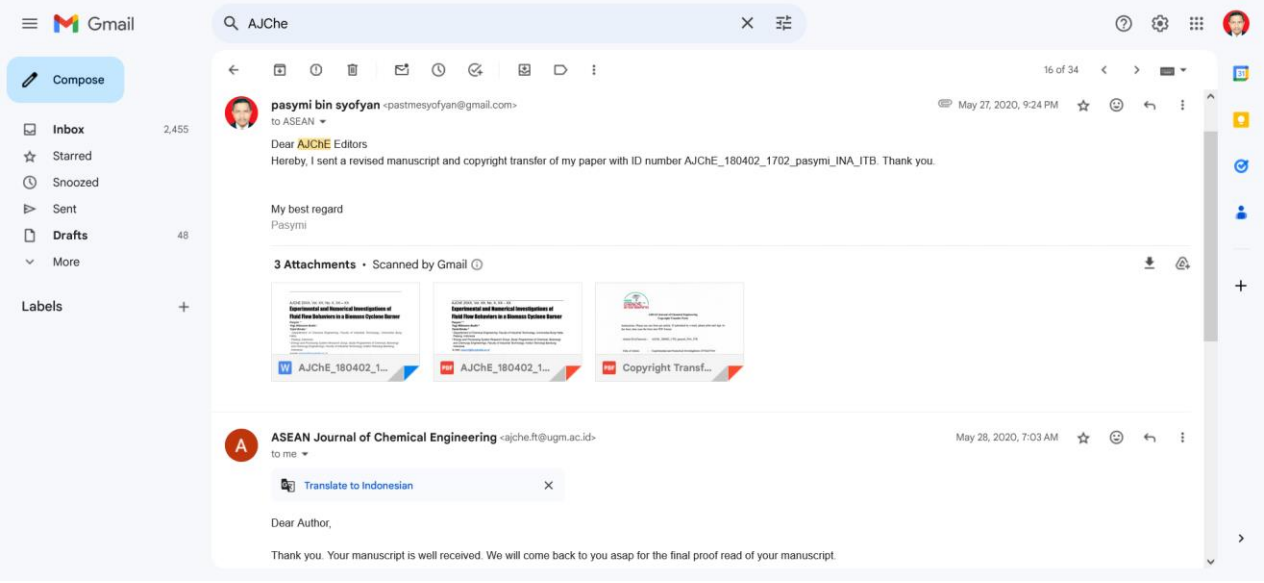
Gmail
AJChe
Compose
Inbox 2,455
Starred
Snoozed
Sent
Drafts 48
More
Labels
16 of 34
pasymi bin syofyan <pastmesyofyan@gmail.com>
to ASEAN
May 27, 2020, 9:24 PM
Dear AJChE Editors
Hereby, I sent a revised manuscript and copyright transfer of my paper with ID number AJChE_180402_1702_pasymi_INA_ITB. Thank you.
My best regard
Pasymi
3 Attachments • Scanned by Gmail
AJChE_180402_1...
AJChE_180402_1...
Copyright Transf...
ASEAN Journal of Chemical Engineering <ajche.ft@ugm.ac.id>
to me
May 28, 2020, 7:03 AM
Translate to Indonesian
Dear Author,
Thank you. Your manuscript is well received. We will come back to you asap for the final proof read of your manuscript.

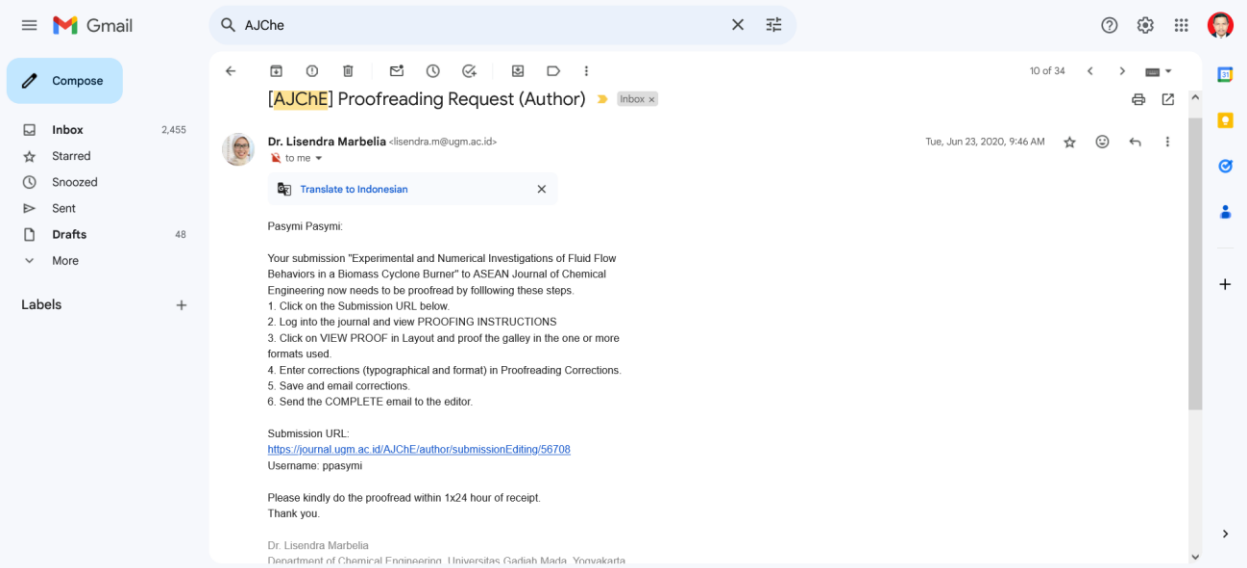
Gmail
AJChe
Compose
Inbox 2,455
Starred
Snoozed
Sent
Drafts 48
More
Labels
10 of 34
[AJChE] Proofreading Request (Author)
Inbox ×
Dr. Lisendra Marbelia <lisendra.m@ugm.ac.id>
to me
Tue, Jun 23, 2020, 9:46 AM
Translate to Indonesian
Pasymi Pasymi:
Your submission "Experimental and Numerical Investigations of Fluid Flow Behaviors in a Biomass Cyclone Burner" to ASEAN Journal of Chemical Engineering now needs to be proofread by folllowing these steps.
1. Click on the Submission URL below.
2. Log into the journal and view PROOFING INSTRUCTIONS
3. Click on VIEW PROOF in Layout and proof the galley in the one or more formats used.
4. Enter corrections (typographical and format) in Proofreading Corrections.
5. Save and email corrections.
6. Send the COMPLETE email to the editor.
Submission URL:
https://journal.ugm.ac.id/AJChE/author/submissionEditing/56708
Username: ppasymi
Please kindly do the proofread within 1x24 hour of receipt.
Thank you.
Dr. Lisendra Marbelia
Department of Chemical Engineering, Universitas Gadjah Mada, Yogyakarta

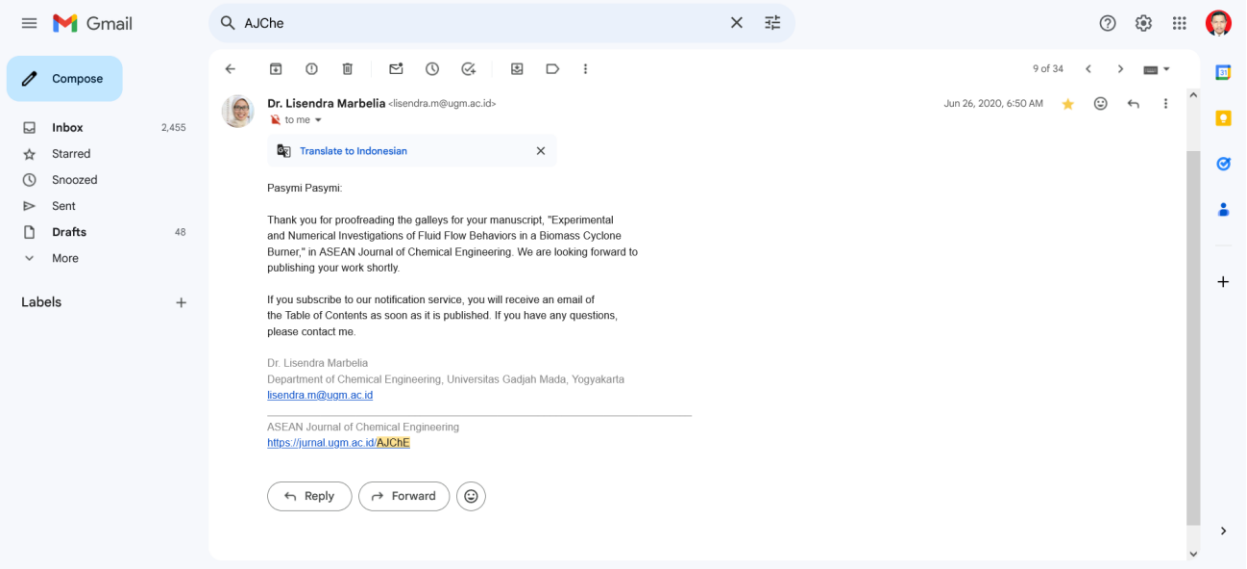
Gmail
AJChe
Compose
Inbox 2,455
Starred
Snoozed
Sent
Drafts 48
More
Labels
9 of 34
Dr. Lisendra Marbelia <lisendra.m@ugm.ac.id>
to me
Jun 26, 2020, 6:50 AM
Translate to Indonesian
Pasymi Pasymi:
Thank you for proofreading the galleys for your manuscript, "Experimental and Numerical Investigations of Fluid Flow Behaviors in a Biomass Cyclone Burner," in ASEAN Journal of Chemical Engineering. We are looking forward to publishing your work shortly.
If you subscribe to our notification service, you will receive an email of the Table of Contents as soon as it is published. If you have any questions, please contact me.
Dr. Lisendra Marbelia
Department of Chemical Engineering, Universitas Gadjah Mada, Yogyakarta
lisendra.m@ugm.ac.id
ASEAN Journal of Chemical Engineering
https://jurnal.ugm.ac.id/AJChE
Reply
Forward

Submitted Article

Original Research Paper

Experimental and Numerical Investigation on Fluid Flow Behaviors in a Biomass Cyclone Burner

Pasymi[1,2], Yogi Wibisono Budhi[1] and Yazid Bindar[1†]

[1] Energy and Processing System Research Group, Study Programmes of Chemical, Bioenergy and Chemurgy Engineerings, Faculty of Industrial Technology, Institut Teknologi Bandung, Indonesia

[2] Department of Chemical Engineering, Faculty of Industrial Technology, Bung Hatta University, Padang, Indonesia

†Corresponding Author Email: yazid@che.itb.ac.id

ABSTRACT

A combination of experimental and numerical method was used to investigate the effects of tangential inlet thickness (R_{IA}) and tangential velocity (I_{IT}) on backflow pattern and pressure drop in a cyclone burner. Both of the fluid flow behaviors greatly influence the burner performance. Experimentally, backflow pattern in the burner was observed through paper slices dynamic in a transparent burner and pressure drop was measured using U-shaped tube manometer. Meanwhile numerically, fluid flow behaviors in the burner was simulated using standard k-ε turbulent model, under Ansys-Fluent software. At certain values of R_{IA} and I_{IT}, experiment results showed indication of backflow formation in the burner. The same backflow phenomenon was also observed in the simulation results. It turned out that, the backflow pattern and position of simulation results are similar to the experiment results, which closely resembles a tornado-tail. The research also indicated that the results of simulated static pressure drop were closely approaching the experiment results, particularly for I_{IT} values ≤ 4.3. Mean deviation of static pressure between the simulation and the experiment results, for varied range of R_{IA} and I_{IT}, was 14.67%. From the results above, it was obvious that backflow pattern and static pressure in cyclone burners are greatly influenced by the R_{IA} and I_{IT} values. In addition, the effect of tangential velocity was more dominant compared to the thickness. For I_{IT} values ≤ 4.3, standard k-ε turbulent model could predict fluid flow behaviors in cyclone burners with a satisfying result.

Keywords: backflow pattern, paper slice dynamic, cyclone burner, initial tangential intensity, inlet aspect ratio, static pressure, standard k-ε turbulent model, tornado-tail

1. INTRODUCTION

Backflow from a furnace to a burner can sustain flame stability in burners. It bring hot combustion gas from the furnace to the burner; therefore, burner temperature is always high and capable of heating and burning incoming fuel (Al Abdeli and Masri 2015). The formation of backflow in a burner is triggered by swirl flow. Its characteristic is influenced by the burner geometry and operating conditions. According to Nemoda, backflow pattern only forms at high swirl number (Sn) $\geq$ 2.48 (Nemoda et al. 2005). On the other hand, Bourgouin reported that backflow pattern and frequency in a gas turbine are determined by the swirler geometry [Bourgouin et al. 2013].

Apart from affecting backflow formation, swirl flow also influences other fluid dynamics characteristic such as mixing intensity, residence time and particle distribution (Pasymi et al. 2017, Arnao et al. 2015). On the other hand, the use of swirl flow also introduces a challenge due to its potential of increasing static pressure in burners (Aydin et al. 2014, Gawali and Bhambere 2015). From the perspective of fluid dynamics, static pressure serves as an obstacle of the fluid flow. The higher the static pressure, the greater the power required to drain the air and fuel into the boiler furnace, resulting in higher burner operating cost.

Although recent studies on swirl flow characteristic have been carried out by previous researchers, supplementary studies are still necessary to be conducted, particularly in lieu of cyclone burners development process using new types of fuel. Non-wood biomass has a great potential to be used as boiler fuel in the future. The physical and chemical characteristics of this biomass are significantly different from coal (Baxter et al. 2005, Vassilev et al. 2015). As a result, the design of geometry and operating conditions of these burner types require separate studies.

The proposed cyclone burner design in this study is dedicated for perennial crop biomass. The geometric design consisted of a cylindrical tube with an axial inlet and a tangential injection inlet. While, the cross-section shape of the axial inlet is a circle, the cross-section shape of the tangential

inlet is rectangular, as shown in Fig. 1. The effects of tangential inlet thickness and tangential inlet velocity on backflow pattern and pressure drop are studied in this research.

2. INVESTIGATION METHODOLOGY

The method used in this study was a combination of experimental and numerical method. The experimental method was carried out under limited conditions and the results were used to validate the simulation results. Meanwhile, numerical method was applied widely until comprehensive data and information were obtained.

2.1 Experimental Set-Up

The experiment to determine backflow pattern and static pressure was conducted in a cyclone burner made of transparent material (acrylic). The burner geometry and *experimental equipment set-up* are given in Fig. 1.

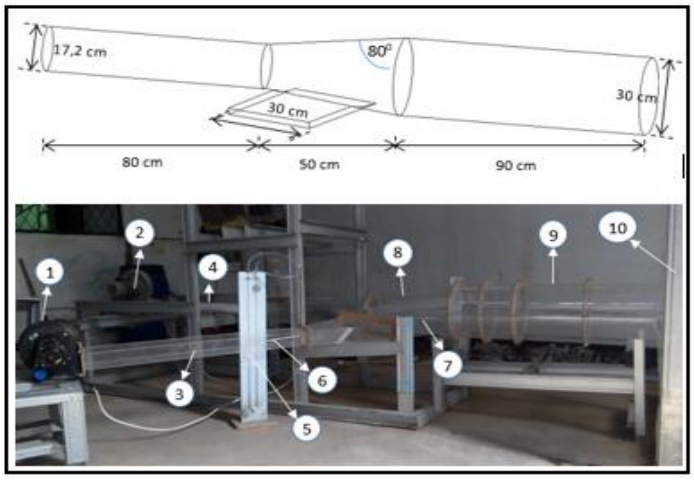

Annotation:

1 = tangential blower
2 = axial blower
3 = tangential inflow
4 = axial inflow
5 = U-shaped manometer
6 = pitot tube
7 = tangential inlet
8 = frustum
9 = burner cylinder
10= furnace box

Fig. 1. Burner geometry and experimental equipment set-up

Backflow pattern in the cyclone burner was observed through paper slices dynamic. Then, it was visualized using a camera. The paper used was bright colour wax paper. This type of paper was chosen due to its low specific gravity and susceptibility toward water vapour. The paper slices

were 10 cm long, 0.5 cm wide and 0.002 cm thick, with an average weight of 0.015 gr per slice. The paper slices were stick on a long thread and installed along y-axis of the burner at a certain z position. To avoid gravitational effect at a particular distance (z), the paper stripes was assembled in horizontal position, as shown in Fig. 2.a.

Meanwhile, static pressure was measured using a U-shaped tube manometer. The static pressure in each end of burner cylinder was extracted through ± 2 mm-diameter-hole, at z = 1.31 and z = 2.19 m. Then, both holes were connected to U-tube filled with water. The water height difference in U-tube was converted to show the static pressure difference in Pascal unit. The set-up of static pressure measurement can be seen in Fig. 2.b.

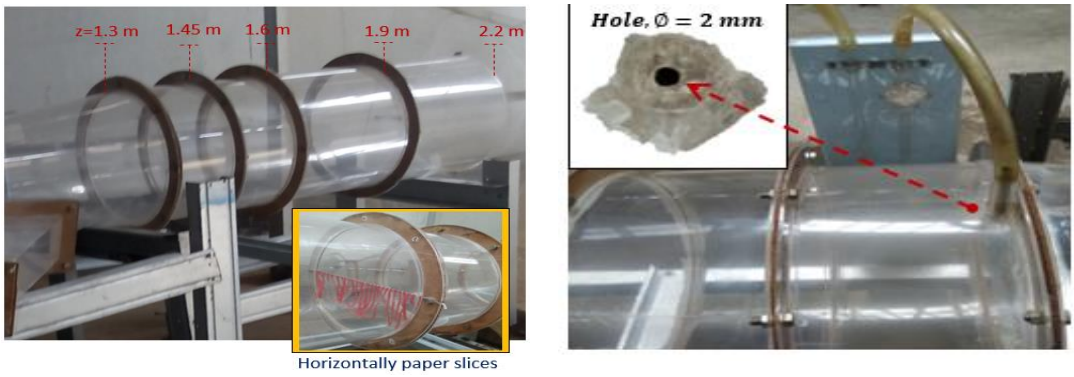

a. Paper slices dynamic determination b. Static pressure meassurement

Fig. 2. Equipment set-up for paper slices dynamic and static pressure determination

Air velocity, both through axial inlet and tangential injection inlet, was determined using pitot tubes. Variation of airflow rate in each inlet was arranged by adjusting blower-opening size.

2.2 Simulation Techniques

Fluid dynamics in this study was simulated using standard k-ε turbulent model. This model has been reported by previous researchers as able to model swirl flow well, particularly for low swirl

flow intensity (Nemoda et al. 2005, pasymi et al. 2017, Vazquez 2012, Reis et al. 2014). These below equations are partial differential equations used in standard k-ε turbulent model (Bindar 2017).

$$\frac{\partial \rho}{\partial t} = \frac{\partial \rho \bar{u}_x}{\partial x} + \frac{\partial \rho \bar{u}_y}{\partial y} + \frac{\partial \rho \bar{u}_z}{\partial z} \quad (1)$$

$$\frac{\partial \rho \bar{u}_i}{\partial t} + \sum_{j=x}^{y,z} \rho \bar{u}_j \frac{\partial \bar{u}_i}{\partial j} = -\frac{\partial \bar{P}}{\partial i} + \sum_{j=x}^{y,z} \frac{\partial}{\partial j}\left[(\mu + \mu_t)\frac{\partial \bar{u}_i}{\partial j}\right] + \rho g_i \quad (2)$$

$$i = x, y, z$$

$$\rho \frac{\partial k}{\partial t} + \sum_{j=x}^{y,z} \rho \bar{u}_j \frac{\partial k}{\partial j} = \sum_{j=x}^{y,z} \frac{\partial}{\partial j}\left[\frac{\mu_{\text{eff}}}{\sigma_{\text{k}}}\frac{\partial k}{\partial j}\right] + G_{\text{k}} - \rho\varepsilon \quad (3)$$

$$\rho \frac{\partial \varepsilon}{\partial t} + \sum_{j=x}^{y,z} \rho \bar{u}_j \frac{\partial \varepsilon}{\partial j} = \sum_{j=x}^{y,z} \frac{\partial}{\partial j}\left[\frac{\mu_{\text{eff}}}{\sigma_{\varepsilon}}\frac{\partial \varepsilon}{\partial j}\right] + C_{\varepsilon 1}\frac{\varepsilon}{k}G_k - C_{\varepsilon 2}\rho\frac{\varepsilon^2}{k} \quad (4)$$

Variable *x*, *y* and *z* on the equations are the direction components of Cartesian coordinate, while $\bar{u}_x$, $\bar{u}_y$, and $\bar{u}_z$ are the average velocity for each of direction component. Variable *k* is the specific turbulent kinetic energy and variable ε is the dissipation rate of the specific turbulent kinetic energy.

The turbulent viscosity (μ_{t}) is formulated by semi empirical equation shown in equation (5). Meanwhile, G_k is production rate of specific turbulent kinetic energy and given by equation (6). Parameter C_{μ}, $C_{\varepsilon 1}$, $C_{\varepsilon 2}$, σ_{k} and σ_{ε} are empirical constants.

$$\mu_t = C_{\mu}\rho(k^2/\varepsilon) \quad (5)$$

$$G_{\text{k}} = 2\mu_{\text{t}}\sum_{j=x}^{y,z}\left(\frac{\partial \bar{u}_j}{\partial j}\right)^2 + \mu_{\text{t}}\left[\left(\frac{\partial \bar{u}_{\text{x}}}{\partial y} + \frac{\partial \bar{u}_{\text{y}}}{\partial x}\right)^2 + \left(\frac{\partial \bar{u}_{\text{x}}}{\partial z} + \frac{\partial \bar{u}_{\text{z}}}{\partial x}\right)^2 + \left(\frac{\partial \bar{u}_{\text{y}}}{\partial z} + \frac{\partial \bar{u}_{\text{z}}}{\partial y}\right)^2\right] \quad (6)$$

Simulation was performed in a steady state condition using Ansys-Fluent software. The wall boundary condition was built based on the assumption of no split condition; therefore, all turbulent

variables (p, u_x, u_y, u_z, k, and ε) on the burner wall are zero. Meanwhile, the turbulent variable value near the wall (at log layer) is determined by a standard wall function.

2.3 Experimental Variables

Tangential inlet thickness in this research is expressed in the form of inlet aspect ratio (R_{IA}). R_{IA} is the ratio between the width to the thickness of the tangential inlet cross-section. Variation in R_{IA} values was arranged by keeping the width value constant while varying tangential inlet thickness. The correspondent width was 30 cm, while the thickness values were 2, 3, and 4.5 cm. As a result, variation of R_{IA} used were 15, 10 and 6.7.

Meanwhile, tangential velocity is expressed in initial tangential intensity (I_{IT}). I_{IT} is calculated based on the equation below (Chen et al. 1999).

$$I_{IT} = \frac{A_c}{A_t}\frac{\dot{m}_t^2}{(\dot{m}_t + \dot{m}_a)^2} \qquad (7)$$

Variable A_c is the cross-sectional area of the burner cylinder and A_t is the cross-sectional area of tangential inlet. Meanwhile, $\dot{m}_a$ and $\dot{m}_t$ are the mass flow rate through axial inlet and tangential inlet, respectively.The higher the I_{IT}, the higher swirl flow intensity would be and vice versa. In this experiment, I_{IT} values were varied between 2.5 – 5.6.

3. RESULTS AND DISCUSSIONS

3.1 The Effect of I_{IT} on Backflow Pattern for Various Values of R_{IA}

3.1.1 Burner with R_{IA} = 15

The simulation result showed that for I_{IT} = 4.6, backflow was formed in the burner. The backflow occurred in the middle of the burner which stretched along the burner cylinder. It flowed continuously as a vortex that resembled a tornado-tail, as shown in Fig. 3.a. Similar phenomenon

also arose for I_{IT} = 2.5, however, shorter backflow penetration was formed for this I_{IT} value. It only occurred along the 2/5-end of the burner cylinder, as shown in Fig. 3.b.

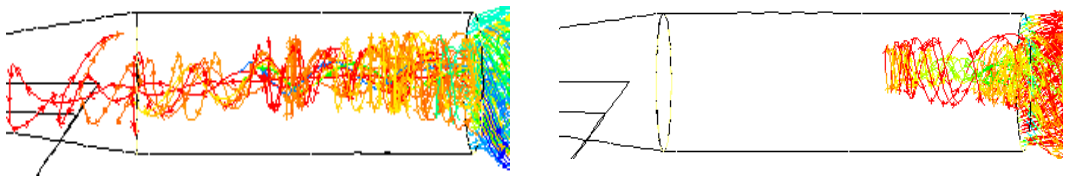

a. For I_{IT} = 4.6 b. For I_{IT} = 2.5

Fig. 3. Backflow pattern that resembles a tornado tail for R_{IA} = 15

The existence of that particular backflow was later tested experimentally through paper slices dynamic experiment, at position z = 1.45 m. For I_{IT} = 4.6, there was an indication of backflow formed in the middle of the burner. This experiment result was in accordance with the simulation results of flow pathlines (Fig. 3.a). The profile of axial velocity vector, as depicted in Fig.4.a, also shows an indication of backflow in the center of the burner, including at z = 1.45 m. The indication of backflow existence was shown by the negative value of axial velocity vector (pointed to the left).

The comparison between the backflow pattern of experiment and simulation result, which was extracted at z = 1.45 m, can be seen in Fig. 4.b. The figure showed that the backflow pattern from simulation result, with standard k-ε turbulent model, was almost identical to the paper slices dynamic experiment result.

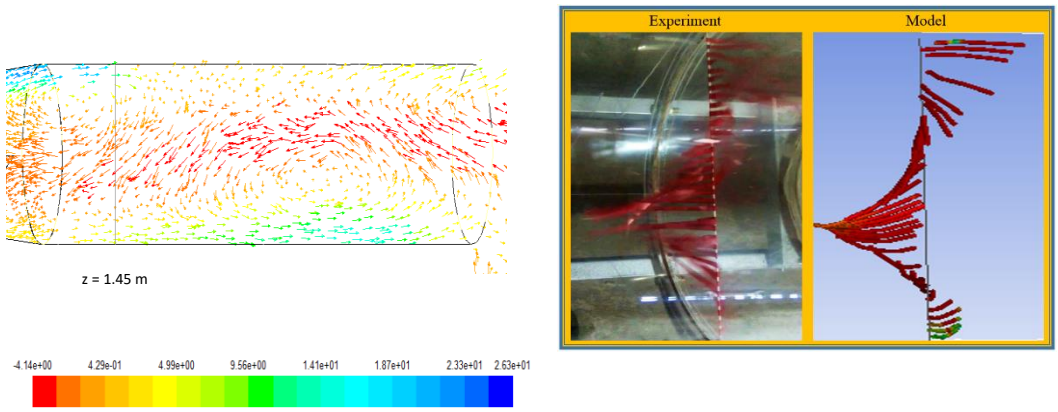

a. Axial velocity vectors

b. Flow pathlines at z = 1.45 m

Fig. 4. Axial velocity profiles and flow pathlines at I_{IT} = 4.6

Meanwhile, for lower flow rate (I_{IT} = 2.5), the experiment result also indicated the formation of backflow at z = 1.45 m. The backflow had smaller intensity compared to the previous one. This result seemed to contradict the result on Fig. 3.b, which showed that no backflow was formed at the z position. This result could be explained from the visualization of axial velocity vector, as depicted in Fig. 5.a. The axial velocity vector distribution, at zx plane, showed two indications of backflows located at the 1/4-start and 2/5-end of the burner cylinder.

The backflow occurred in the first 1/4 length of burner cylinder was called internal recirculation flow. On the other hand, backflow formed in the 2/5-end of burner cylinder length was called external backflow. The later was responsible for sustaining flame stability because, it would bring hot flue gas from the furnace into the burner to maintain burner temperature high (Al-Abdeli and Masri 2015).

Figure 5.a shows that at z = 1.45 m, there were some axial velocity vectors directed to the left. This indicated the formation of backflow at that particular position in the form of internal recirculation flow. That backflow phenomenon was the one that was recorded by paper slices

dynamic experiment. The simulation result with fluid release line at z = 1.45 m also revealed a formation of low intensity backflow. The comparison of backflow patterns of simulation and experiment result, at z = 1.45 m, were depicted in Fig. 5.b. It is clearly seen that both patterns showed high level of adequate similarity.

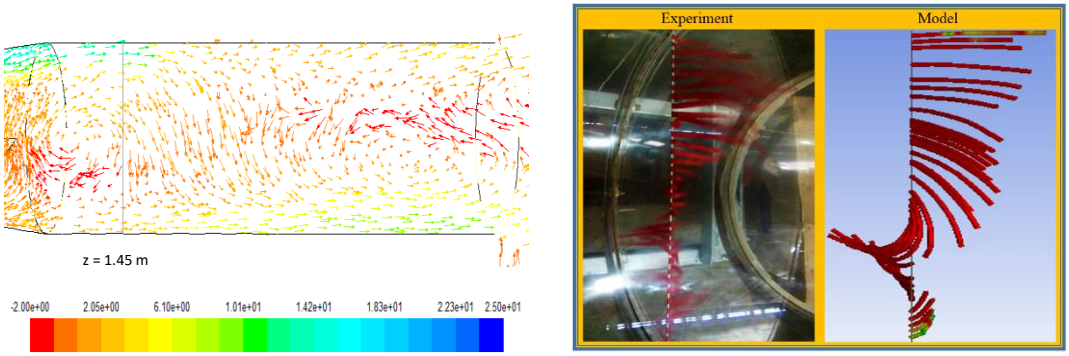

a. Axial velocity vectors b. Flow pathlines at z = 1.45 m

Fig. 5. Axial velocity profiles and flow pathlines at I_{IT} = 2.5

3.1.2 Burner with R_{IA} = 10

At I_{IT} = 5.3, backflow with a tornado-tail like pattern was found to penetrate along the burner cylinder, as depicted in Fig. 6.a. While, at lower I_{IT} value of 2.8, the backflow pattern only penetrated along the 1/3-end of burner cylinder, as shown in Fig. 6.b.

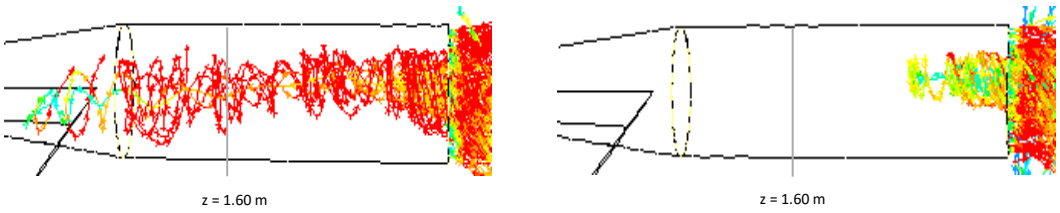

a. For I_{IT} = 5.3 b. For I_{IT} = 2.8

Fig. 6. Backflow patterns that resembles a tornado tail for R_{IA} = 10

Although for I_{IT} = 5.3 the experiment of paper slices dynamic visualization showed a formation of backflow at z = 1.6 m, but for I_{IT} = 2.8 the backflow was not formed at all. These experiment results were in line with the simulation results of backflows. Fig.6.b shows that there is no backflows, at z = 1.6 m. The conformity of flow pathlines between experiment and simulation results is shown in Fig. 7.

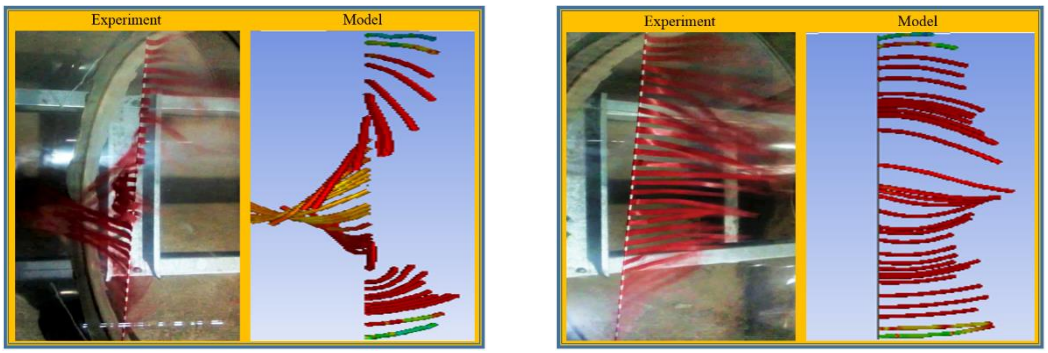

a. For I_{IT} = 5.3 b. For I_{IT} = 2.8

Fig. 7. Comparison of flow pathlines of experiment and simulation for R_{AI} = 10

3.1.3 Burner with R_{IA} = 6.7

The simulation result, for I_{IT} = 5.3, indicated the formation of backflow that penetrated along 2/3-end of the burner cylinder, shown in Fig. 8.a. This was supported by the experiment result that showed the indication of backflow at z = 1.90 m. The comparison of paper slices dynamic visualization and the simulation result is given in Fig. 9.a.

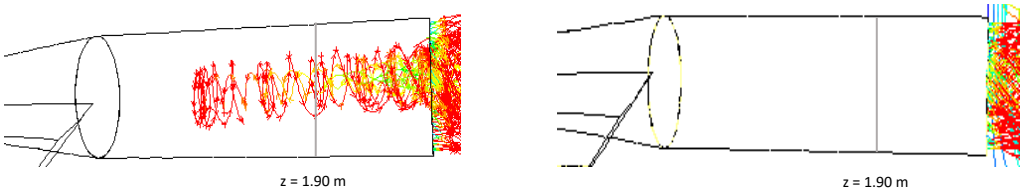

a. For I_{IT} = 5.3 b. For I_{IT} = 2.9

Fig. 8. Backflow patterns that resembles a tornado tail for R_{IA} = 6.67

For I_{IT} = 2.9, the simulation result did not show any backflow formation along the burner cylinder, as seen in Fig. 8.b. Nonexistence of backflow for that particular condition was also supported by the paper slices dynamic experiment result. Also at z = 1.9 m, the experiment did not indicate backflows formation, as shown in Fig. 9.b.

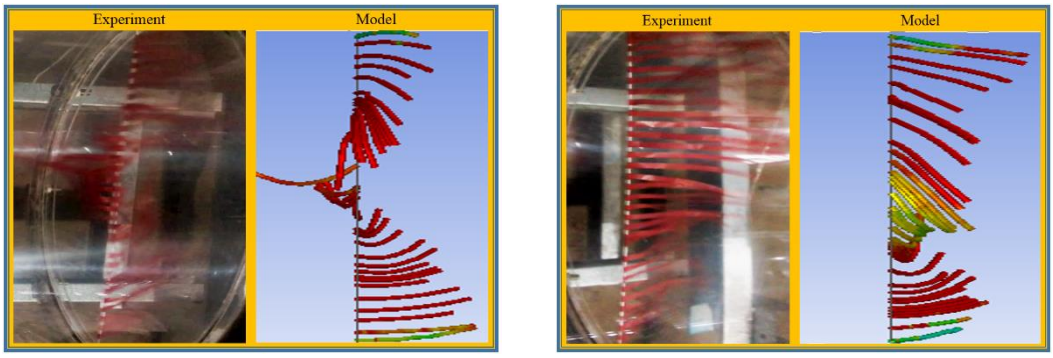

a. For I_{IT} = 5.3 b. For I_{IT} = 2.9

Fig. 9. Comparison of flow pathlines of experiment and simulation for R_{AI} = 6.67

From various simulation conditions above, it was found that backflow patterns of simulation results were similar with experiment results of paper slices dynamic. It can be concluded that standard k-ε turbulent model was able to predict the formation of backflow pattern in a cyclone burner well. Simulation results also showed that backflow pattern in the burner was greatly influenced by tangential velocity (I_{IT}) and tangential inlet thickness (R_{IA}). This is consistent with Nemoda and Bourgoin's finding (Nemoda et al. 2005, Bourgouin et al. 2015).

3.2 The Effect of R_{IA} and I_{IT} to Static Pressure

Static pressure difference along a burner cylinder is caused by kinetic energy dissipation rate (epsilon) as a result of friction loss. Kinetic energy dissipation dominantly occurs in the area near the burner's wall. Therefore, static pressure measurement is conducted on that particular area.

3.2.1 The Effect of I_{IT} to Static Pressure

Experiment results showed that the higher the I_{IT}, the bigger the difference in static pressure along the burner cylinder would be. Similar result was achieved from the simulation using standard k-ε turbulent model. Mean deviation of the static pressure from simulation results compared to experiments results, for R_{IA} 15, 10 and 6.7, were 10, 14 dan 20%, respectively. The comparison of static pressure drop profile for several R_{IA} and I_{IT} values is shown in Fig. 10. The difference between the simulation results to the experiment results increased with the rise of I_{IT}. For $I_{IT} \leq 4.3$, the deviation was under 20%. This is similar to previous studies which state that, for low swirl intensity, standard k-ε turbulent model can satisfactorily model swirl flow well [Nemoda et al. 2005, Pasymi et al. 2017, Vazquez 2012).

For $I_{IT} > 4.3$, the difference between simulation results and experiment results were higher. This happened because for high values of $I_{IT,}$ the swirl flow tends to be non-isotropic, with different turbulent strength penetrating to all direction components (Jakirlic et al. 2002). Meanwhile, standard k-ε turbulent model is built based on the isotropic turbulent assumption, where turbulent velocity is considered uniform to every direction. It is why, isotropic assumption is difficult to accept for turbulent swirl flow, particularly for high swirl intensity.

Dependency of the pressure drop to the tangential velocity (I_{IT}) can be explained as follow; (1) for high values of I_{IT}, the tangential velocity in the inlet burner would be high, (2) on the contrary, the static pressure on that position would be low, (3) due to kinetic energy dissipation from friction

loss along the burner cylinder, the tangential velocity toward the burner outlet would decrease, (4) on the other hand, the kinetic energy dissipation rate (epsilon) and the pressure drop along the burner cylinder would grow. Therefore, the greater the value of I_{IT}, the greater the pressure drop along the burner cylinder was and vice versa.

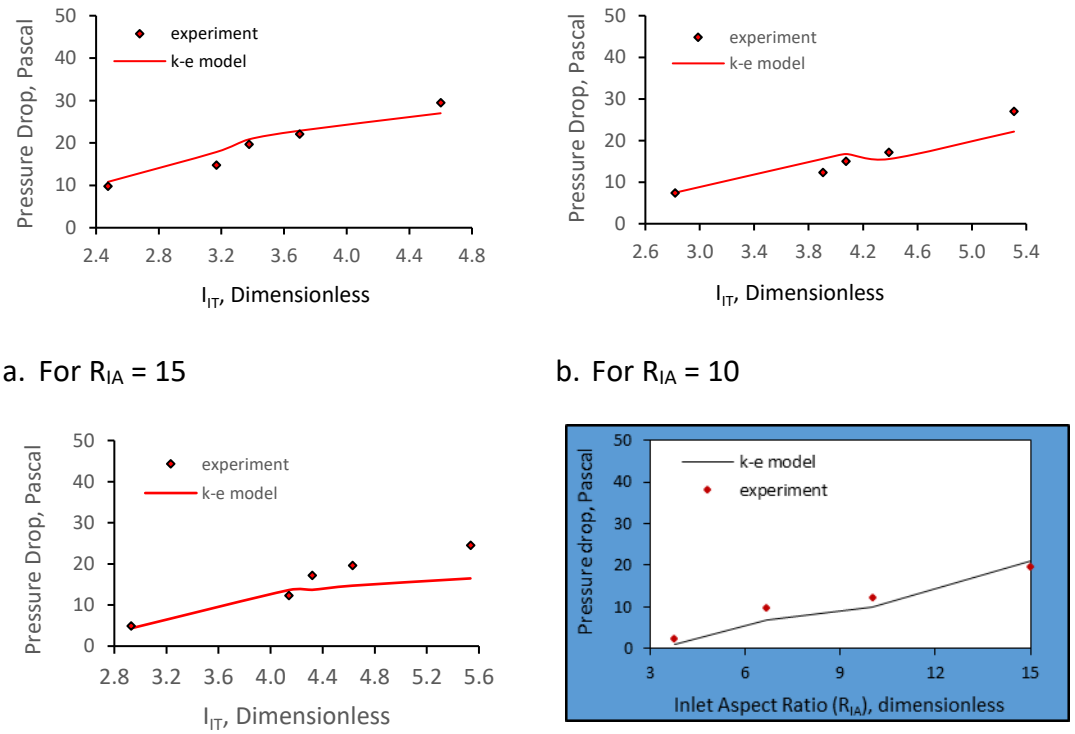

Fig. 10. Static pressure drop profile in the burner for various I_{IT} and R_{IA}

3.2.2 The Effect of R_{IA} to Static Pressure

Both experiment and simulation results indicated that the static pressure loss in the burner was directionally proportional to the inlet aspect ratio (R_{IA}). The greater the value of R_{IA}, the greater static pressure difference in the burner was. The comparison between simulation and experiment

result, for I_{IT} = 3.4, is depicted in Fig. 10.d. The pressure drop from the simulation result deviated ± 27% from the experiment result.

The difference in R_{IA} would affect tangential inlet cross-sectional area. The thinner the tangential inlet thickness (the bigger the R_{IA}), the smaller the cross-sectional area of tangential inlet would be and the higher the tangential velocity would be. This leads to the higher kinetic energy dissipation rate (epsilon) and the pressure drop would be. As a result, the bigger R_{IA} would result in the bigger pressure drop.

4. CONCLUSION

Standard k-ε turbulent model could be use to predict backflow pattern and static pressure profile in cyclone burners satisfactorily well, particularly for $I_{IT} \leq 4.3$. The backflow patterns from simulation results were highly similar with experiment results of paper slices dynamic. The formed backflow patterns closely resembled to a tornado tail. Mean deviation of pressure drop from simulation and experiment results, for varied range of R_{IA} and I_{IT}, was 14.67%.

Simulation results also revealed that backflow pattern and pressure drop profile in cyclone burners were greatly influenced by tangential inlet thickness and tangential velocity. More precisely, the effect of tangential velocity was more dominant compared to the thickness. For the same value of thickness (R_{IA}), backflow intensity was directly proportional to initial tangential intensity (I_{IT}). The higher the tangential velocity, the greater the backflow intensity was. The same phenomenon applied to pressure drop; the higher the tangential velocity, the greater the pressure drop was. This happened as a result of high pressure loss due to friction loss with burner wall.

Acknowledgments

We would like to thank the expertise group of research directorate of ITB for the funding support provided to the implementation of this research through P3MI scheme.

REFERENCES

Al-Abdeli, Y. M. & Masri, A. R. (2015). Review of laboratory swirl burners and experiments for model validation. *Exp. Therm. Fluid Sci.,* 69, 178-196.

Arnao, J.H.S., Ferreira, D.J.O., Santos, C.G., Alvarez, J.E., Rangel, L.P. & Park, S.W. (2015). The influence of swirl burner geometry on the sugar-cane bagasse injection and burning. *International Journal of Mechanical, Aerospace, Industrial, Mechatronic and Manufacturing Engineering*, 9, 798-801.

Aydin, O., Avci, M., Markal, B. & Yazici, Y. (2014). An experimental study on the decaying swirl flow in a tube. *Int. Commun. Heat Mass*, 55, 22-28.

Baxter, L., Ip, L., Lu, H. & Tree, D. (2005). Distinguishing biomass combustion characteristics and their implications for sustainable energy. *The 5th Asia Pacific Conference on Combustion,* University of Adelaide, Australia.

Bindar, Y. (2017). *Rekayasa komputasi aliran turbulen multidimensi*, First edition. ITB Press, Bandung, Indonesia.

Bourgouin, J.F., Moeck, J., Durox, D., Schuller, T., & Candel, S. (2013). Sensitivity of swirling flows to small changes in the swirler geometry. *CR Mecanique,* 341, 211–219.

Chen, J., Haynes, B.S. & Fletcher, D.F.A. (1999). Numerical and experimental study of tangentially injected swirling pipe flows. *International Conference on CFD in the Minerals and Process Industries CSIRO*, Melbourne, Australia, 2, 485-490.

Gawali, S. S. & Bhambere, M. B. (2015). Computational fluid dynamics approach for predictions of cyclone separator pressure drop. *IJMERR*, 4 (1), 374-377.

Jakirlic, S., Hanjalic, K. & Tropea, C. (2002). Modelling rotating and swirling turbulent flows: A perpetual challenge. *AIAA J*, 40, 1984-1996.

Nemoda, S., Bakic, V., Oka, S., Zivkovic, G. & Crnomarkavic, N. (2005). Experimental and numerical investigation of gaseous fuel combustion in swirl chamber. *Int. J. Heat Mass Tran.*, 48, 4623–4632.

Pasymi, Budhi, Y.W. & Bindar, Y. (2017). Effect of initial tangential intensity on the fluid dynamic characteristics in tangential burner. *MATEC Web Conf.*, 101, 1-6.

Reis, L.C.B.S., Carvalho, J.A.Jr., Nascimento, M.A.R., Rodrigues, L.O., Dias, F.L.G. & Sobrinho, P.M. (2014). Numerical modeling of flow through an industrial burner orifice. *Appl. Therm. Eng.*, 67, 201-213.

Vassilev, S.V., Vassileva, C.G. & Vassilev, V.S. (2015). Advantages and disadvantages of composition and properties of biomass in comparison with coal: An overview. *Fuel*, 158, 330–350.

Vazquez, J. A. R. (2012). A computational fluid dynamics investigation of turbulent swirling burner. *Thesis*, University of Zaragoza, Spain.

AJChE 20XX, Vol. XX, No. X, XX – XX

Experimental and Numerical Investigations of Fluid Flow Behaviors in a Biomass Cyclone Burner

Pasymi [*,1]
Yogi Wibisono Budhi [2]
Yazid Bindar [2]

[1] *Departement of Chemical Engineering, Faculty of Industrial Technology, Universitas Bung Hatta, Padang, Indonesia*
[2] *Energy and Processing System Research Group, Study Programmes of Chemical, Bioenergy and Chemurgy Engineerings, Faculty of Industrial Technology, Institut Teknologi Bandung, Indonesia*
[*] *e-mail:* pasymi@bunghatta.ac.id

A combination of the experimental and numerical methods was used to investigate the fluid flow behaviors in a proposed cyclone burner. Recirculation flow and pressure drop, two of the important fluid flow behaviors that affect the burner's performance, have been studied here. Experimentally, the recirculation flow phenomenon in the burner was observed through paper slices dynamic in a transparent burner, and pressure drop was measured using a tube manometer. Meanwhile numerically, the fluid flow behaviors were simulated using the standard k-ε turbulence model, under Ansys-Fluent software. The simulation results showed that, at a certain value of inlet aspect ratio (R_{IA}) and initial tangential intensity (I_{IT}), especially for high I_{IT}, the recirculation flow phenomenon was clearly observed in the center of the burner cylinder which closely resembles a tornado-tail. The indication of existence recirculation flow was also found from the experiment results. The study also exhibited that the results of simulated static pressure drop were closely approaching the experiment results, particularly for I_{IT} values ≤ 4.3. The mean deviation of static pressure between the simulation and the experiment results, for a varied range of R_{IA} and I_{IT}, was about 15%. From the results above, it was obvious that fluid flow behaviors (recirculation flow and static pressure) in the proposed cyclone burner are greatly influenced by the R_{IA} and I_{IT} values, where the I_{IT} effect was more significant compared to the R_{IA}. This study also suggests that, the standard k-ε turbulence model could be relied upon to well predict the behaviors of fluid flow in the proposed cyclone burner, at low to moderate swirl intensities.

Keywords: Recirculation flow, Paper slice dynamic, Cyclone burner, Initial tangential intensity, Inlet aspect ratio, Static pressure, Standard k-ε turbulence model, Tornado-tail

INTRODUCTION

Recirculation flow from a furnace to a burner can sustain flame stability in the burner, especially for the solid-fueled burner. It brings hot combustion gas from the furnace to the burner; therefore, burner temperature is always high and capable of heating and burning incoming fuel (Al Abdeli and Masri 2015).

The formation of recirculation flow in any type of chamber has been studied by several researchers. They revealed that the recirculation flow trigger is the swirl flow.

The effect of chamber geometry on the swirl flow behaviors has been studied by Bourgouin et al. (2013), Arnao, et al. (2015), and Ziqiang et al. (2016). While, the effect of chamber operating condition on swirl flow behaviors has been studied by Nemoda (2005), and Pasymi et al. (2018). They state that, in general, recirculation flow is formed at moderate to high swirl intensities.

Apart from affecting recirculation flow formation, swirl flow also influences other fluid dynamics characteristics such as mixing intensity, residence time, pressure drop, and particle distribution (Arnao et al. 2015, Pasymi et al. 2017). The use of swirl flow introduces a challenge due to its potential of increasing static pressure in the burner (Aydin et al. 2014, Gawali and Bhambere 2015).

From the perspective of fluid dynamics, static pressure serves as an obstacle to the fluid flow. The higher the static pressure, the greater the power required to drain the air and fuel into the boiler furnace, resulting in a higher burner operating costs. A compromise of the swirl intensity value must be found where the recirculation flow can be formed while the pressure drop can be obtained as low as possible.

Although there have been many studies on swirl flow behaviors by researchers, supplementary studies are still necessary to be conducted, in order to develop new types of the burner. One of the potential new burners is a light biomass burner. Light biomass has great potential to be used as boiler fuel in the future. The physical and chemical characteristics of this biomass are significantly different from coal (Baxter et al. 2005, Vassilev et al. 2015). As a result, the design of geometry and operating conditions of this burner type requires separate studies.

The proposed cyclone burner design in this study is dedicated to light biomass. The geometric design consisted of a cylindrical tube with an axial inlet and a tangential injection inlet. The cross-section shape of the axial inlet is a circle and the cross-section shape of the tangential inlet is rectangular, as shown in Fig. 1.

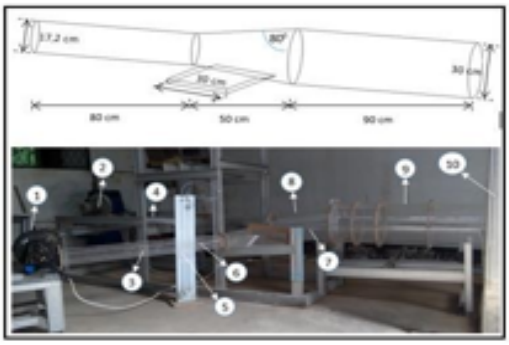

Annotation:

1 = tangential blower	6 = pitot tube
2 = axial blower	7 = tangential inlet
3 = tangential inflow	8 = frustum
4 = axial inflow	9 = burner cylinder
5 = U-shaped manometer	10= furnace box

Fig. 1: Burner geometry and experimental equipment set-up

This research aims to study the effects of tangential inlet thickness and velocity on the formation of recirculation flow and pressure drop profile in the proposed cyclone burner. In addition, this study is also intended to evaluate whether the standard k-ε turbulent model can predict satisfactorily the swirl flow behaviors in the burner.

INVESTIGATION METHODOLOGY

The method used in this study was a combination of the experimental and numerical methods. The experimental method was carried out under limited conditions and the results were used to validate the simulation results. Meanwhile, the numerical method was applied widely until comprehensive data and information were obtained.

Experimental Set-Up

The experiment to determine the recirculation flow pattern and static pressure profile were conducted in a cyclone burner made of transparent material (acrylic). The burner geometry and experimental equipment set-up are given in Fig. 1.

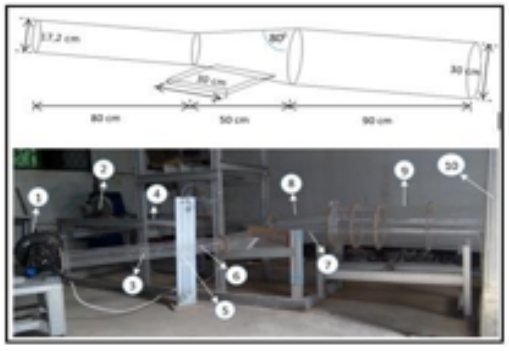

Annotation:

1 = tangential blower	6 = pitot tube
2 = axial blower	7 = tangential inlet
3 = tangential inflow	8 = frustum
4 = axial inflow	9 = burner cylinder
5 = U-shaped manometer	10= furnace box

Fig. 1: Burner geometry and experimental equipment set-up

In this experiment, the recirculation flow pattern in the cyclone burner was observed through paper slices dynamic. Then, it was visualized using a camera. The paper used was a bright color wax paper. This type of paper was chosen due to its low specific gravity and susceptibility toward water vapor. The paper slices were 10 cm in length, 0.5 cm in wide, and 0.002 cm in thickness, with an average weight of 0.015 gr per slice. The paper slices were stick on a long thread and installed along the y-axis of the burner at a certain z position. To avoid the gravitational effect at a particular distance (z), the paper stripes were assembled in a horizontal position, as shown in Fig. 2.a.

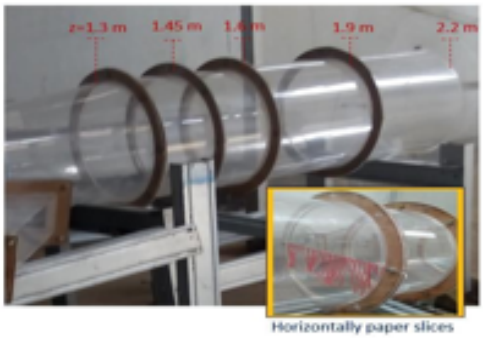

a. Paper slices dynamic determination

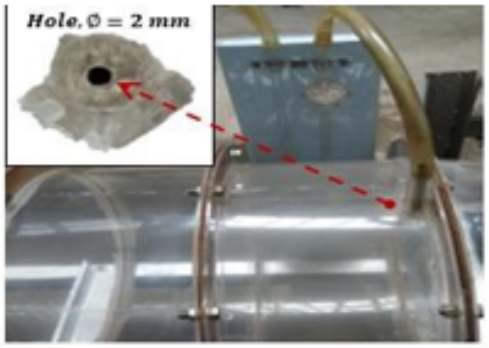

b. Static pressure meassurement

Fig. 2: Experimental equipment set-up

Meanwhile, static pressure was measured using a U-shaped tube manometer. The static pressure at each end

of the burner cylinder was extracted through ± 2 mm-diameter-hole, at z = 1.31 and z = 2.19 m. Then, both holes were connected to U-tube filled with water. The water height difference in U-tube was converted to show the static pressure difference in the Pascal unit. The set-up of static pressure measurement can be seen in Fig. 2.b.

Air velocity, both through axial and tangential inlets, was determined using a pitot tube. Variation of airflow rate in each inlet was arranged by adjusting the blower-opening size.

Simulation Techniques

Numerically, fluid dynamics in this study was simulated using the standard k-ε turbulence model. This model has been reported by previous researchers is able to model swirl flow well, particularly for low swirl flow intensity (Nemoda et al. 2005, Vazquez 2012, Reis et al. 2014, Pasymi et al. 2017). These below equations are partial differential equations used in the standard k-ε turbulence model (Bindar 2017).

$$\frac{\partial \rho}{\partial t} = \frac{\partial \rho \bar{u}}{\partial x} + \frac{\partial \rho \bar{v}}{\partial y} + \frac{\partial \rho \bar{w}}{\partial z} \quad (1)$$

$$\frac{\partial \rho \bar{u}_i}{\partial t} + \sum_{j=x}^{y,z} \rho \bar{u}_j \frac{\partial \bar{u}_i}{\partial x_j} = -\frac{\partial \bar{p}}{\partial x_i} + \sum_{j=x}^{y,z} \frac{\partial}{\partial x_j}\left[(\mu + \mu_t)\frac{\partial \bar{u}_i}{\partial x_j}\right] + \rho g_i \quad (2)$$

where $i = x, y, z$

$$\rho \frac{\partial k}{\partial t} + \sum_{j=x}^{y,z} \rho \bar{u}_j \frac{\partial k}{\partial x_j} = \sum_{j=x}^{y,z} \frac{\partial}{\partial x_j}\left[\frac{\mu_{eff}}{\sigma_k}\frac{\partial k}{\partial x_j}\right] + G_k - \rho\varepsilon \quad (3)$$

$$\rho \frac{\partial \varepsilon}{\partial t} + \sum_{j=x}^{y,z} \rho \bar{u}_j \frac{\partial \varepsilon}{\partial x_j} = \sum_{j=x}^{y,z} \frac{\partial}{\partial x_j}\left[\frac{\mu_{eff}}{\sigma_\varepsilon}\frac{\partial \varepsilon}{\partial x_j}\right] + C_{1\varepsilon}\frac{\varepsilon}{k}G_k - C_{2\varepsilon}\rho\frac{\varepsilon^2}{k} \quad (4)$$

Variables *x*, *y*, and *z* on the equations are the direction components of the Cartesian coordinate, while $\bar{u}$, $\bar{v}$, and $\bar{w}$ are the average velocity for each direction component. Variable *k* is the specific turbulent kinetic energy and ε is the dissipation rate of the specific turbulent kinetic energy.

The turbulent viscosity (μ_t) is formulated by the semi-empirical equation shown in equation (5). Meanwhile, G_k is the production rate of specific turbulent kinetic energy and given by equation (6). Parameters C_μ, $C_{\varepsilon 1}$, $C_{\varepsilon 2}$, σ_k, and σ_ε are the empirical constants.

$$\mu_t = C_\mu \rho (k^2/\varepsilon) \quad (5)$$

$$G_k = 2\mu_t \sum_{j=x}^{y,z} \left(\frac{\partial \bar{u}_j}{\partial x_j}\right)^2 + \mu_t \left|\frac{\partial \bar{u}}{\partial y} + \frac{\partial \bar{v}}{\partial x}\right|^2 + \left|\frac{\partial \bar{u}}{\partial z} + \frac{\partial \bar{w}}{\partial x}\right|^2 + \left|\frac{\partial \bar{v}}{\partial z} + \frac{\partial \bar{w}}{\partial y}\right|^2 \quad (6)$$

The simulation was performed in a steady-state condition using Ansys-Fluent software. The wall boundary condition was built based on the assumption of no split condition. Therefore, all turbulent variables ($\bar{p}$, $\bar{u}$, $\bar{v}$, $\bar{w}$, *k*, and ε) on the burner wall are zero. Meanwhile, the turbulent variable's value near the wall (at the log layer) is determined by a standard wall function.

Research Variables

There are two research variables investigated here, those are tangential inlet thickness and tangential inlet velocity. Tangential inlet thickness is expressed in the form of inlet aspect ratio (R_{iA}), which is the ratio between the width to the thickness of the tangential inlet cross-section, as given in Equation (7).

$$R_{IA} = \frac{t}{a} \quad (7)$$

Variation in R_{IA} values was arranged by keeping the width value constant while varying tangential inlet thickness. The correspondent width was 30 cm, while the thickness values were 2, 3, and 4.5 cm. As a result, the variation of R_{IA} used was 15, 10, and 6.7.

Meanwhile, tangential velocity is expressed as initial tangential intensity (I_{IT}). Initial tangential intensity is calculated based on the equation below (Chen et al. 1999).

$$I_{IT} = \left(\frac{\dot{m}_t}{\dot{m}_c}\right)^2 \left(\frac{A_c}{A_t}\right)^2 \quad (8)$$

Variable A_c is the cross-sectional area of the burner cylinder and A_t is the cross-sectional area of the tangential inlet. Meanwhile, $\dot{m}_c$ and $\dot{m}_t$ are the mass flow rate through the burner cylinder and tangential inlet, respectively. The higher the I_{IT}, the higher the swirl flow intensity would be, and vice versa. In this experiment, I_{IT} values were varied between 2.5 – 5.6.

RESULTS AND DISCUSSION

The Effect of I_{IT} on Recirculation flow Pattern for Various Values of R_{IA}

The effect of I_{IT} on recirculation flow is discussed in 3 groups, namely for R_{IA} values of 15, 10, and 6.7. Each group will simultaneously discuss research results, experimentally and numerically.

Burner with R_{IA} = 15

The simulation result showed that for I_{IT} = 4.6, recirculation flow was formed in the burner. The recirculation flow occurred in the middle of the burner which stretched along with the burner cylinder. It flowed continuously as a vortex that resembled a tornado-tail, as shown in Fig. 3.a. A similar phenomenon also arose for I_{IT} = 2.5, however, shorter recirculation flow penetration was formed for this I_{IT} value. It only occurred along the 2/5-end of the burner cylinder, as shown in Fig. 3.b.

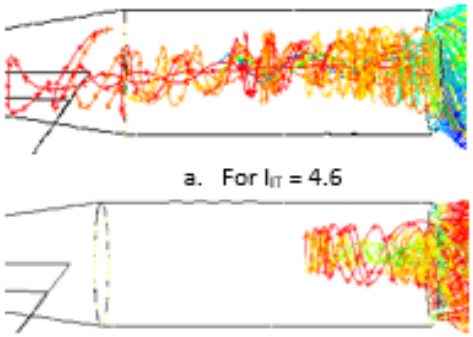

a. For I_{IT} = 4.6

b. For I_{IT} = 2.5

Fig. 3: Recirculation flow patterns for I_{IT} = 4.6 and 2.5 at R_{IA} = 15

The profile of axial velocity vector, as depicted in Fig.4.a, also shows an indication of recirculation flow in the center of the burner. The indication of recirculation flow existence was shown by the negative value of axial velocity vector (pointed to the left).

The existence of that particular recirculation flow was later evaluated experimentally through paper slices dynamic experiment, at position z = 1.45 m. For I_{IT} = 4.6, there was an indication of recirculation flow formed in the middle of the burner. It can be observed from the presence of paper slices in the middle of the burner flowing upside down, as shown on the left of Fig. 4.b. This shows that there

is a match between the simulation results with the experimental ones.

The comparison between flow pathlines from experiment and simulation results, which was extracted at z = 1.45 m, can be seen in Fig. 4.b. The figure showed that the flow pathlines from simulation result, with standard k-ε turbulence model was almost identical to the paper slices dynamic experiment result.

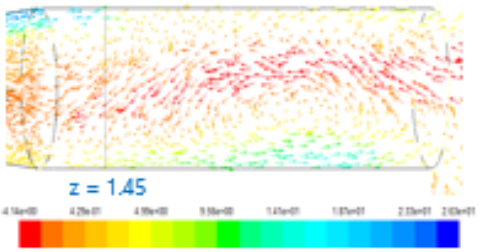

a. Axial velocity vectors

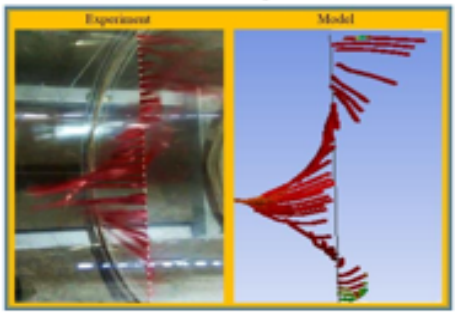

b. Flow pathlines at z = 1.45 m

Fig. 4: Axial velocity profiles and flow pathlines at I_{IT} = 4.6

For lower velocity (I_{IT} = 2.5), the experiment result also indicated the formation of recirculation flow at z = 1.45 m, as shown in Fig. 5.b. The recirculation flow had smaller intensity compared to the previous one. This result seemed to contradict the result in Fig. 3.b, which showed that no recirculation flow was formed at the z position. This result could be explained from the visualization of the axial velocity vector, as depicted in Fig. 5.a. The axial velocity vector distribution, at zx plane, showed two indications of recirculation flows located at the 1/4-start and 2/5-end of the burner cylinder.

The recirculation flow occurred in the first 1/4 length of the burner cylinder was called internal recirculation flow. On the other hand, recirculation flow formed in the 2/5-end of burner cylinder length was called external recirculation flow. The later was responsible for sustaining flame stability because it would bring hot flue gas from the furnace into the burner to maintain burner temperature high (Al-Abdeli and Masri 2015).

Figure 5.a shows that at z = 1.45 m, there were some axial velocity vectors directed to the left. This indicated the formation of recirculation flow at that particular position in the form of internal recirculation flow. That recirculation flow phenomenon was the one that was recorded by paper slices dynamic experiment. The simulation result with fluid release line at z = 1.45 m also revealed a formation of low-intensity recirculation flow. The comparison of recirculation flow patterns of simulation and experiment results, at z = 1.45 m, were depicted in Fig. 5.b. It is clearly seen that both patterns showed a high level of adequate similarity.

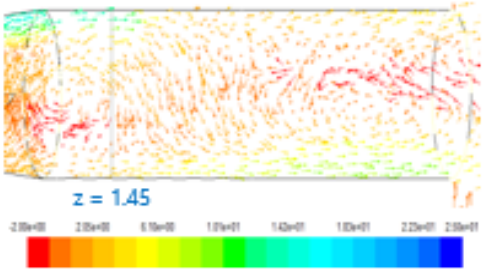

a. Axial velocity vectors

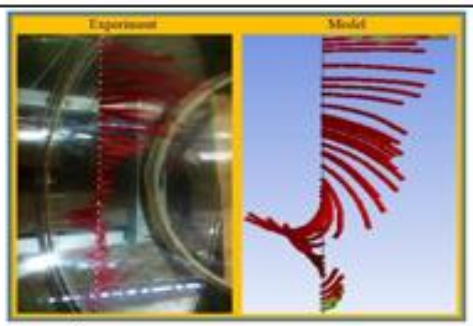

b. Flow pathlines at z = 1.45 m

Fig. 5: Axial velocity profiles and flow pathlines at R_{IA} = 15 and I_{IT} = 2.5

Burner with R_{IA} = 10

Numerically, at I_{IT} = 5.3, recirculation flow with a tornado-tail like pattern was found to penetrate along the burner cylinder, as depicted in Fig. 6.a. While, at lower I_{IT} value of 2.8, the recirculation flow pattern only penetrated along the 1/3-end of burner cylinder, as shown in Fig. 6.b.

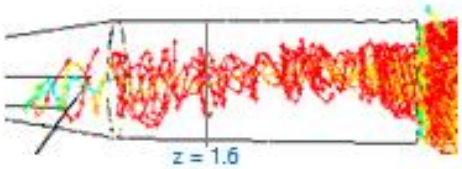

a. For I_{IT} = 5.3

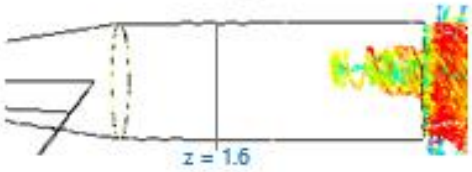

b. For I_{IT} = 2.8

Fig. 6: Recirculation flow patterns for I_{IT} = 5.3 and 2.8 at R_{IA} = 10

Experimentally, the existence of recirculation flow was evaluated at z = 1.6 m. For IIT = 5.3, the indication of recirculation flow was found, while for IIT = 2.8, there was no indication of recirculation flow at all. These findings were in line with the simulation results as in Fig. 6.

The Fig. 7.a indicates the existence of recirculation flow at z = 1.6 m and I_{IT} =5.3, experimentally, and numerically. While Fig. 7.b indicates no recirculation flow indication at lower I_{IT} value (2.8).

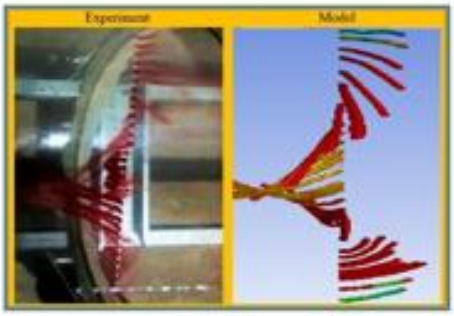

a. For I_{IT} = 5.3

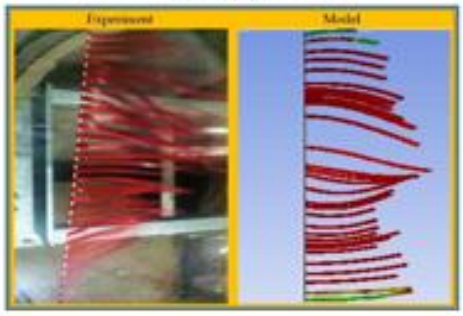

b. For I_{IT} = 2.8

Fig. 7: Comparison of flow pathlines from experiment and simulation at R_{AI} = 10

Burner with R_{IA} = 6,67

The simulation result, for I_{IT} = 5.3, indicated the formation of recirculation flow that penetrated along 2/3-end of the burner cylinder, as shown in Fig. 8.a. This was supported by the experiment result that showed the indication of recirculation flow at z = 1.90 m. The comparison of paper slices dynamic visualization and the

simulation result is given in Fig. 9.a.

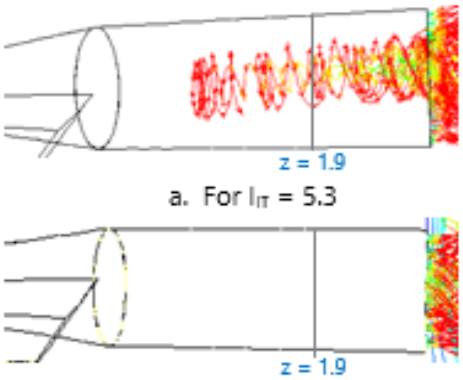

a. For I_{IT} = 5.3

b. For I_{IT} = 2.9

Fig. 8: Recirculation flow patterns for I_{IT} = 5.3 and 2.9 at R_{IA} = 6.67

For I_{IT} = 2.9, the simulation result did not show any recirculation flow indication along the burner cylinder, as seen in Fig. 8.b. The absence of recirculation flow indication under this condition is also shown by the result of dynamic experiment of paper slices at z = 1.9 m, as shown in Fig. 9.b.

From various operating conditions above, it was found that recirculation flow patterns of simulation results were similar with experiment results of paper slices dynamic. It may be said that standard k-ε turbulence model was able to well predict the existence of recirculation flow pattern in a cyclone burner. Simulation results also showed that recirculation flow pattern in the burner was greatly influenced by tangential velocity (I_{IT}) and tangential inlet thickness (R_{IA}). This is consistent with Nemoda and Bourgoin's finding (Nemoda et al. 2005, Bourgouin et al. 2015).

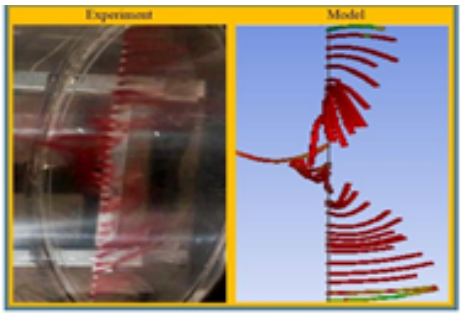

a. For I_{IT} = 5.3

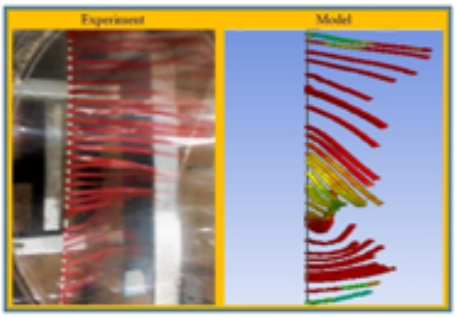

b. For I_{IT} = 2.9

Fig. 9: Comparison of flow pathlines of experiment and simulation at R_{AI} = 6.67

The Effect of R_{IA} and I_{IT} to Static Pressure

Static pressure difference along a burner cylinder is caused by the kinetic energy dissipation rate (epsilon) as a result of friction loss. Kinetic energy dissipation dominantly occurs in the area near the burner's wall. Therefore, static pressure measurement is conducted in that particular area.

The Effect of I_{IT} to Static Pressure

Experiment results showed that the higher the I_{IT}, the bigger the difference in static pressure along the burner cylinder would be. A similar result was achieved from the simulation using standard k-ε turbulence model. Mean deviation of the static pressure from simulation results compared to experiments results, for R_{IA} 15,

10 and 6.7, were 10, 14 dan 20%, respectively. The comparison of static pressure drop profile for several R_{IA} and I_{IT} values is shown in Fig. 10. The difference between the simulation results to the experiment results increased with the rise of I_{IT}. For $I_{IT} \leq 4.3$, the deviation was under 20%. This is similar to previous studies which state that, for low swirl intensity, standard k-ε turbulence model can satisfactorily model swirl flows well [Nemoda et al. 2005, Pasymi et al. 2017, Vazquez 2012).

For $I_{IT} > 4.3$, the difference between simulation results and experiment results were higher. This happened because, for high values of I_{IT}, the swirl flow tends to be non-isotropic, with different turbulent strength penetrating to all direction components (Jakirlic et al. 2002). Meanwhile, standard k-ε turbulence model is built based on the isotropic turbulent assumption, where turbulent velocity is considered uniform in every direction. It is why, the isotropic assumption is difficult to accept for turbulent swirl flow, particularly for high swirl intensity.

The dependency of the pressure drop to the tangential velocity (I_{IT}) can be explained as follow; (1) for high values of I_{IT}, the tangential velocity in the inlet burner would be high, (2) on the contrary, the static pressure on that position would be low, (3) due to kinetic energy dissipation from friction loss along with the burner cylinder, the tangential velocity toward the burner outlet would decrease, (4) on the other hands, the kinetic energy dissipation rate (epsilon) and the pressure drop along the burner cylinder would grow. Therefore, the greater the value of I_{IT}, the greater the pressure drop along the burner cylinder would be and vice versa.

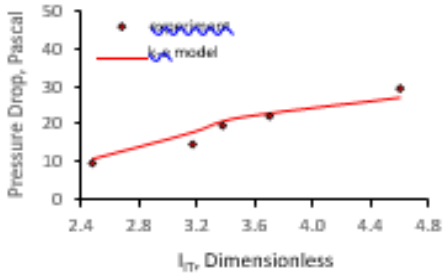

a. For R_{IA} = 15

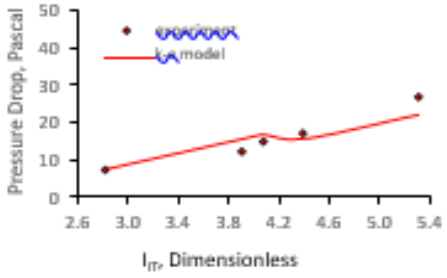

b. For R_{IA} = 10

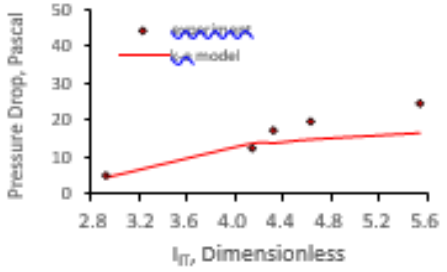

c. For R_{IA} = 6.67

Fig. 10: Profiles of static pressure drop In the burner for various I_{IT} values

The Effect of R_{IA} to Static Pressure

Both experiment and simulation results indicated that the static pressure loss in the burner was directionally proportional to the inlet aspect ratio (R_{IA}). The greater the value of R_{IA}, the greater static pressure difference in the burner would be. The comparison between simulation and experiment result, for I_{IT} = 3.4, is depicted in Fig. 11. In

average, the pressure drop from the simulation result deviated ± 27% from the experiment ones.

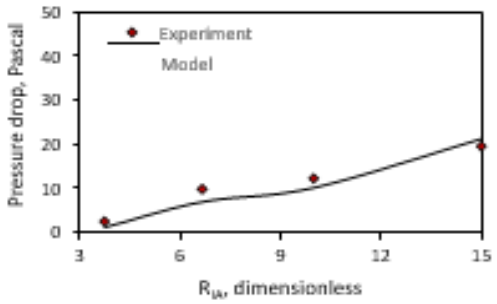

Fig. 11: Profiles of static pressure drop in the burner for various R_{IA} values

The difference in R_{IA} would affect the tangential inlet cross-sectional area. The thinner the tangential inlet thickness (the bigger the R_{IA}), the smaller the cross-sectional area of tangential inlet would be, and the higher the tangential velocity would be. This leads to the higher kinetic energy dissipation rate (epsilon) and the pressure drop would be. As a result, the bigger R_{IA} would result in a bigger pressure drop.

CONCLUSIONS

Experimental and simulation results revealed that the recirculation flow phenomenon was greatly influenced by initial tangential intensity (I_{IT}) and inlet aspect ratio (R_{IA}). The higher the I_{IT}, the higher the swirl flow intensity, and the greater the potential for recirculation flow to form. The formation of the recirculation flow is also directly proportional to the R_{IA}. The recirculation flow patterns formed in the burner closely resembled a tornado tail. The same trend also occurs to the pressure drop; the higher the I_{IT} and R_{IA}, the greater the pressure drop produced and vice versa.

From all experiments and simulations carried out, there was a match between both results for the phenomenon of recirculation flow and the pressure drop profile. The recirculation flow patterns from simulation results were highly similar to the results of the experiment of paper slices dynamic. Furthermore, the mean deviation of pressure drop from simulation and experiment ones, for a varied range of R_{IA} and I_{IT}, was relatively low (about 15%). It may almost be stated that the standard k-ε turbulence model could predict the recirculation flow pattern and static pressure profile in the proposed cyclone burner satisfactorily well, particularly for $I_{IT} \leq 4.3$.

ACKNOWLEDGMENT

We would like to thank the expertise group of research directorates of ITB for the funding support provided to the implementation of this research through the P3MI scheme.

NOMENCLATURE

d	:	tangential inlet thickness [m]
g	:	acceleration gravity [m s^{-2}]
l	:	Tangential inlet width [m]
$\bar{p}$	:	mean static pressure [Pascal]
ρ	:	density [kg m^{-3}]
μ	:	dynamics viscosity [kg m^{-1} s^{-1}]
μ_{eff}	:	effective viscosity [kg m^{-1} s^{-1}]
t	:	time [s]

REFERENCES

1. Al-Abdeli, Y. M., and Masri, A. R. (2015). "Review of laboratory swirl burners and experiments for model validation," *Exp. Therm. Fluid Sci., 69*, 178-196.
2. Arnao, J.H.S., Ferreira, D.J.O., Santos, C.G., Alvarez, J.E., Rangel, L.P., and Park, S.W. (2015). "The influence of swirl burner geometry on the sugar-cane bagasse injection and burning," *International Journal of Mechanical, Aerospace, Industrial, Mechatronic and Manufacturing Engineering, 9*, 798-801.
3. Aydin, O., Avci, M., Markal, B., and Yazici, Y. (2014). "An experimental study on the decaying swirl flow in a tube," *Int. Commun. Heat Mass, 55*, 22-28.
4. Baxter, L., Ip, L., Lu, H., and Tree, D. (2005). "Distinguishing biomass combustion characteristics and their implications for sustainable energy," *The 5th Asia Pacific Conference on Combustion,* University of Adelaide, Australia.
5. Bindar, Y. (2017). *Rekayasa komputasi aliran turbulen multidimensi,* First edition, ITB Press, Bandung, Indonesia.
6. Bourgouin, J.F., Moeck, J., Durox, D., Schuller, T., and Candel, S. (2013). "Sensitivity of swirling flows to small changes in the swirler geometry," *CR Mecanique, 341*, 211–219.
7. Chen, J., Haynes, B.S., and Fletcher, D.F.A. (1999). "Numerical and experimental study of tangentially injected swirling pipe flows," *The 2nd International Conference on CFD in the Minerals and Process Industries CSIRO,* Melbourne, Australia, 485 – 490.
8. Gawali, S. S., and Bhambere, M. B. (2015). "Computational fluid dynamics approach for predictions of cyclone separator pressure drop," *IJMERR, 4 (1)*, 374-377.
9. Jakirlic, S., Hanjalic, K., and Tropea, C. (2002). "Modelling rotating and swirling turbulent flows: A perpetual challenge," *AIAA J, 40*, 1984-1996.
10. Nemoda, S., Bakic, V., Oka, S., Zivkovic, G., and Crnomarkavic, N. (2005). "Experimental and numerical investigation of gaseous fuel combustion in swirl chamber," *Int. J. Heat Mass Tran., 48*, 4623–4632.
11. Pasymi, Budhi, Y.W., and Bindar, Y. (2017). "Effect of initial tangential intensity on the fluid dynamic characteristics in tangential burner," *MATEC Web Conf., 101*, 1-6.
12. Pasymi, Budhi, Y.W., and Bindar, Y. (2018). "Three dimensional cyclonic turbulent flow structures at various geometries, inlet-outlet orientations, and operating conditions," *Journal of Mechanical Engineering and Sciences, 12 (4)*, 4300-4328.
13. Reis, L. C. B. S., Carvalho, J. A. Jr., Nascimento, M.A.R., Rodrigues, L.O., Dias, F.L.G., and Sobrinho, P.M. (2014). "Numerical modeling of flow through an industrial burner orifice," *Appl. Therm. Eng., 67*, 201-213.
14. Vassilev, S.V., Vassileva, C.G., and Vassilev, V.S. (2015). "Advantages and disadvantages of composition and properties of biomass in comparison with coal: An overview," *Fuel, 158*, 330–350.
15. Vazquez, J. A. R. (2012). A computational fluid dynamics investigation of turbulent swirling

burner, *Thesis,* University of Zaragoza, Spain.

16. Ziqiang, L.V., Guangqiang, L., and Yingjie, L. (2016). "Optimization Study on Bias Angle of a Swirl Burner with Tangential Inlet Air," *International Journal of Smart Home, 10*, 171-180.

ASEAN Journal of Chemical Engineering
Copyright Transfer Form

Instructions: Please use one form per article. If submitted by e-mail, please print and sign on the form, then scan the form into PDF format.

Article ID (if known)	:	AJChE_180402_1702_pasymi_INA_ITB
Title of Article	:	Experimental and Numerical Investigations of Fluid Flow Behaviors in a Biomass Cyclone Burner
Author(s)	:	Pasymi, Yogi Wibisono Budhi, dan Yazid Bindar

Agreement on the Copyright Transfer

The undersigned agrees to transfer all copyright rights in and to the above work to the ASEAN Journal of Chemical Engineering (AJChE)'s Editorial Board so that AJChE's Editorial Board shall have the right to publish the work for non-profit use in any media or form. In return, authors retain: (1) all proprietary rights other than copyright; (2) re-use of all or part of the above paper in their other work; (3) right to reproduce or authorize others to reproduce the above paper for authors' personal use or for company use if the source and AJChE's copyright notice is indicated, and if the reproduction is not made for the purpose of sale.

Name (in print) Pasymi

Authorized signature
(Or for joint work, as Agent for all authors)

Name of Employer (in print, if any): Universitas Bung Hatta

Please submit completed copyright form to ajche.ft@ugm.ac.id